ACTA PHYSICA DEBRECINA XLVII, 203 (2013)

DETERMINATION OF BEAM PARAMETERS AT THE NEW IN-AIR MICRO-BEAM SETUP IN ATOMKI

Zs. Török

Institute for Nuclear Research, Hungarian Academy of Sciences Laboratory of Ion Beam Applications, H-4001 Debrecen, P.O. Box 51, Hungary

Abstract

An external nuclear scanning microbeam setup has been installed as the extension of the vacuum chamber of the nuclear microprobe at Atomki, Debrecen. The expected beam characteristics for the new in-air setup are presented in this paper. The energy loss and scattered beam dimensions under different conditions were calculated using SRIM2011 and PRAM codes. Finally the beam dimension at a given adjustment was determined experimentally, too.

I. Introduction

Ion beam analytical (IBA) techniques such as particle induced X-ray emission (PIXE) [1], particle induced gamma emission (PIGE), Rutherford backscattering spectrometry (RBS) or scanning transmission ion microscopy (STIM) are frequently used to determine the elemental composition of samples in various multidisciplinary fields [2]. In scanning nuclear microprobes a focused ion beam is used in combination with the above mentioned complementary IBA techniques enabling the quantitative characterization of samples on microscopic scale.

The Scanning Nuclear Microprobe in Debrecen [3] has been extensively used since its installation in 1993 for analytical purposes in materials sciences [4], biology [5], medicine [6], aerosol science [7], geology [8], archaeometry

[9] and for lithography [10]. All these measurements and irradiations were performed under high vacuum conditions.

Recently, as part of an infrastructure development program of the Hungarian Academy of Sciences an external microbeam setup was installed at the Debrecen Scanning Nuclear Microprobe Facility. The aim of the development was to be able to analyse such samples which cannot be placed in the vacuum chamber due to either their size, fragility or other reasons. An external setup has many advantages, e.g. easy sample positioning, no heat and charging effects on the samples, so it is preferred by lot of laboratories who work in the field of characterization of archaeological and museum objects [11].

The microbeam was planned that way that the minimum beam size (1μm x 1μm) can be achieved in the middle of the vacuum chamber. The external setup moves the focus point 37 cm away from the centre of the chamber. Therefore the broadening of the beam is expected. In addition the energy and size of the beam spot on the target are also affected by the scattering on the window material and the path covered by the beam in the atmosphere.

In this work I determine the expected beam characteristics (size, energy) under different conditions (exit beam energy, exit window material and thickness, the distance travelled in air or in helium atmosphere, etc.), and finally I present experimental results on the determination of the beam size on the new setup.

II. Experimental setup

The scanning proton microprobe was built up on the 0° beam line of the 5 MV Van de Graaff accelerator of Atomki. The external microbeam add-on system by Oxford Microbeams [12] was mounted after the vacuum chamber, as shown in Figure 1 and 2.

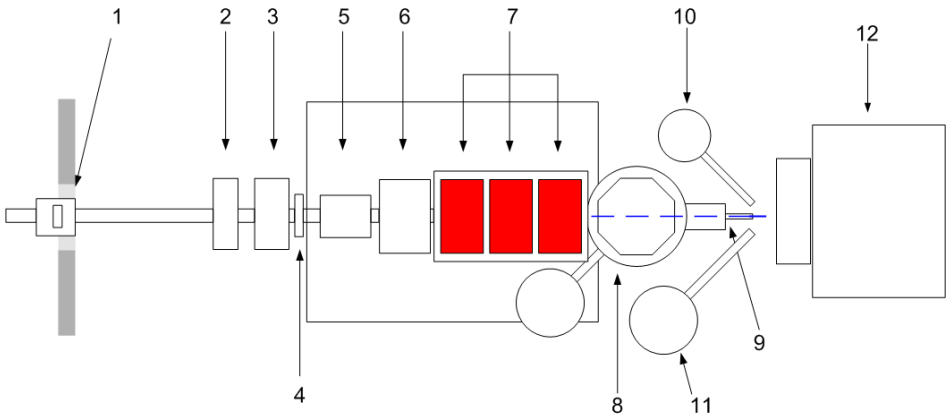

Figure 1: Schematic plan view of the external beam set-up at Atomki: (1) object slits, (2) pneumatic valve, (3) quartz viewer, (4) fast valve, (5) collimator slits, (6) scanning coils, (7) quadrupole triplet, (8) vacuum chamber, (9) exit nozzle with 2 lasers, (10) SDD X-ray detector, (11) Si(Li) X-ray detector, (12) precision XYZ-stage

The aperture of the object slit serves as an object to be demagnified by a lens system (in this case a quadruple triplet). By the help of scanning coils the focused beam spot is moved over the surface of the sample.

The system is equipped with two X-ray detectors at 135° on both sides of the beam. For measuring the light elements (Na-Zn) a silicon drift detector (SDD) with an 8 μm thick Be window is used. A permanent magnet with 1 Tesla magnetic field is protecting the detector from the scattered protons. On the other side a Si(Li) detector with 50 mm^2 active area and with a 25 μm thick Be window is installed. A 125 μm thick Kapton foil is used as an absorber before the detector.

For easy and reproducible positioning on the sample two alignment lasers, a digital microscope and a computer controlled precision XYZ stage are used. With the help of these equipments it is easy to move the samples with several micrometers step size.

Exit windows with different thicknesses and of different materials can be used according to the actual demands. Currently Kapton foils of 8 μm thickness and Silicon-Nitride (Si_3N_4) films with 100 nm, 200 nm and 500 nm thickness

are available in our Laboratory. The geometry of this system determines that the target should be placed 3, 4 or 5 mm from the exit window. If needed, the volume between the exit window and the target, as well as the volume between the target and the SDD detector can be flooded with He.

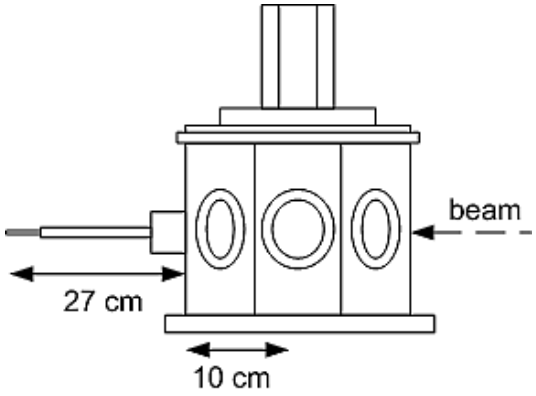

Figure 2: Schematic side view of the vacuum chamber and the exit nozzle.

III. Results

III.1 Calculation of the spot size

In the vacuum chamber a beam size about 1 micrometer can be achieved in both directions. However, since the focus point is moved by a significant amount (37 cm), the minimum size of the beam spot will be bigger.

In order to determine the beam dimensions, I calculated the theoretical beam size at the end of the nozzle using the ion optics computer code Pram [13]. The theoretical beam size together with the input parameters is shown in Table 1. The results show that the adjustments of the vacuum setup mismatch to the external setup. The shape of the geometric beam spot transforms to rectangular instead of square. To keep the square shape the settings of the object and/or the collimator slits must be changed. With different object aperture setting ($\Delta x = 100$, $\Delta y = 50$) I got the result of the square shape: 5.5×5.5 μm^2. These new adjustment are ideal to be applied for the external setup.

Table 1: Optical beam parameters at the end of exit nozzle using a usual in-vacuum setting

Proton beam energy	2 MeV
Object distance	5.88 m
Image distance	60.7 cm
X, Y demagnification	18.5, 9.7
Collimator slit aperture setting ($\Delta x,\Delta y$)	800 x 800 μm^2
Object aperture setting ($\Delta x,\Delta y$)	200, 50μm
Beam size in vacuum	*2.5 x 2.5 μm^2*
Calculated geometric beam spot size at the end of the exit nozzle	11 x 5.5 μm^2

III.2 Beam dimensions in atmosphere

In external setups, before reaching the target, particles are delivered in air through a thin foil. As in earlier studies [12, 14, 15] it was described the gas surrounding the target increases the beam dimensions and the energy loss of the beam. Flowing helium between the exit window and sample, as well as between the sample and the detector decreases the straggling, the energy loss and the absorption of the low-energy emitted X-rays.

Widely used exit window materials are the Kapton foil and the Silicon-Nitride (Si_3N_4) films. I calculated the beam scattering and the energy loss for different circumstances with the help of the SRIM 2011 (the Stopping and Range of Ions in Matter) program code [16]. Table 2 shows the calculations for 3 MeV protons travelling through 2, 3, 4 and 5 mm air and He after Kapton and Silicon-Nitride foils. I used the beam diameter containing 75% of the total flux (d_{75}) assuming a Gaussian profile. This value is approximately 20% larger than the full width at half maximum (FWHM) [12].

Table 2 indicates that at thin windows (such as Si_3N_4) the broadening of the beam diameter is dominated by the external path in atmosphere while for

thicker windows (such as Kapton) the most important effect is due to the scattering in the foil.

Table 2: The energy loss (keV) and the scattered beam dimension (d_{75} in μm) for different distances between exit window and the target. The initial energy of the proton beam is 3 MeV.

	2mm		**3mm**		**4mm**		**5mm**	
in air	**keV**	**μm**	**keV**	**μm**	**keV**	**μm**	**keV**	**μm**
8 μm Kapton	150	39	162	64	176	86	187	101
200 nm Si_3N_4	30	13	42	23	53	33	66	44
100 nm Si_3N_4	27	11	39	19	51	30	64	39
in He								
8 μm Kapton	129	35	131	59	134	81	136	101
200 nm Si_3N_4	9	9	12	16	14	20	16	25
100 nm Si_3N_4	7	7	11	9	11	14	13	18

For our first measurements we used 200 nm thick Si_3N_4 foil which has very good mechanical resistance and radiation hardness [11] while the straggling effect and energy loss remains at minimum.

According to the different measurement and irradiation tasks different beam energies and different beams were used. In Table 3 I show the results of the calculations for 2, 2.5, 3, 3.5 MeV H^+ and 2 MeV He^+ beam using 200 nm thick Silicon-Nitride film as exit window material and 3 mm external path in atmosphere.

Table 3: The energy loss (keV) and the scattered beam dimension (d_{75} in μm) for different beam energies using 200nm Si_3N_4 window material and 3 mm external path. 'None' gives the scattering due to the window alone.

	None	**in air**		**in He**	
	keV	**keV**	**μm**	**keV**	**μm**
2 MeV He^+	62	605	83	164	45
2 MeV H^+	7	56	34	16	23
2.5 MeV H^+	6	47	30	13	19
3 MeV H^+	5	42	23	12	16
3.5 MeV H^+	4	37	19	10	13

III.3 Measured beam size

I measured the beam size on a copper mesh grid with 250 micron lattice constant. The exit window material was 200 nm thick Si_3N_4 film, the target was placed 3 mm from the window and we used a H^+ beam with 2.5 MeV energy. The broadening effect, caused by the air particles, can be clearly seen in the maps (Fig. 3). The beam diameter (d_{75}) was found to be $32\times35\mu m^2$ in air and $30\times33\mu m^2$ in He atmosphere. These dimensions are in good agreement with the calculated ones of $35\times35\mu m^2$ in air but the theoretical beam size in He atmosphere is smaller: $25\times25\mu m^2$. It is shown that the satisfactory He saturation was not achieved [17].

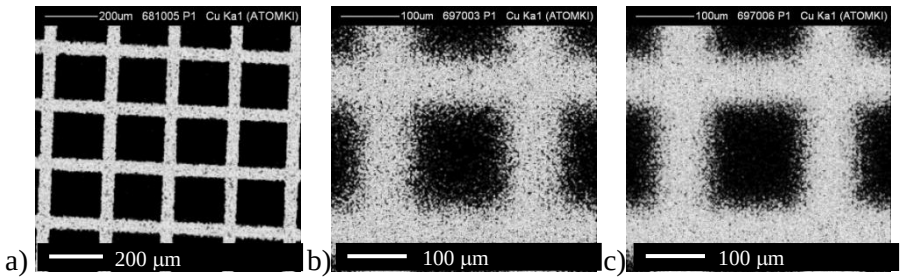

Figure 3: Maps of the Cu grid in vacuum (a), air (b) and in He (c).

IV. Summary

In this paper I presented theoretical calculations and experimental determination of the beam parameters at the new external microbeam setup of Atomki for different circumstances. I showed that the calculated beam sizes were in good agreement with the measured ones for a given beam energy and a given external path. Therefore it can be assumed that the other calculated results would also give good match with the experimental data. The knowledge of these expected beam characteristics is essential for planning any experiment, i.e. to choose the irradiating particle, the beam energy, the window material and thickness, the atmosphere and the window-target distance.

Acknowledgement

The work is supported by the TÁMOP-4.2.2/B-10/1-2010-0024 project. The project is co-financed by the European Union and the European Social Fund. The development of the new in-air microbeam system was partially financed by the Hungarian Academy of Sciences in the frame of an infrastructure development project in 2010-2011.

References

[1] E. Koltay, *Ionokkal keltett Auger-elektronok és röntgen sugárzás*. Akadémiai kiadó, Budapest, 1992

[2] C. Jeynes, M.J. Bailey, N.J. Bright, M.E. Christopher, G.W. Grime, B.N. Jones, V.V Palistin, R.P. Webb, Nucl. Instr. and Meth. B. **271** (2012) 107-118

[3] I. Rajta, I. Borbély Kiss, Gy. Mórik, L. Bartha, E. Koltay, Á.Z. Kiss, Nucl. Instr. and Meth. B. **109/110** (1996) 148-153

[4] I. Rajta, G.A.B. Gál, S.Z. Szilasi, Z. Juhász, S Biri, M Mátéfi-Tempfli, S. Mátéfi-Tempfli, Nanotechnology **21** (2010)29:5704(4)

[5] Z. Szikszai, Zs. Kertész, I. Kocsár, V. Oláh, Acta Biologica Szegediensis **52** (2008)81-83.

[6] Z. Szikszai, Zs. Kertész, E. Bodnár, I. Major, I. Borbíró, Á.Z. Kiss, Hunyadi J., Nucl. Instr. and Meth. B. **268** (2010)2160-2163

[7] Zs. Kertész, Z. Szikszai, Z. Szoboszlai, A. Simon, R. Huszánk, I. Uzonyi, Nucl. Instr. and Meth. B **267** (2009)2236-2240

[8] Z. Szoboszlai, Zs. Kertész, Z. Szikszai, I. Borbély-Kiss, E. Koltay, Nucl. Instr. and Meth. B **267** (2009)12-13:2241-2244

[9] A. Simon, H. Matiskainen, I. Uzonyi, L. Csedreki, Z. Szikszai, Zs. Kertész, Raisanen J., Kiss Á. Z., X-Ray Spectrometry **40** (2011)3:224-228

[10] S.Z. Szilasi, R. Huszánk, D. Szikra, T. Váczi, I. Rajta, I. Nagy, Materials Chemistry and Physics **130** (2011)702-707

[11] L. Giuntini, Anal Bioanal Chem **401** (2011) 785-793

[12] G.W. Grime, M.H. Abraham, M.A. Marsh, Nucl.Instr. and Meth. B.**181** (2001) 66-70

[13] M.B.H. Breese, D.N. Jamieson, P.J.C King, *Materials analysis using a nuclear microprobe*, John Wiley&Sons, New York, 1996 (Chapter 3).

[14] M. Massi, L. Giuntini, M. Chiari, N. Gelli, P.A. Mandò, Nucl.Instr. and Meth. B. **190** (2002) 276-282

[15] J. Salomon, J.-C. Dran, T. Guillou, B. Moignard, L. Pichon, P. Walter, F. Mathis, Nucl.Instr. and Meth. B. **266** (2008) 2273-2278

[16] *SRIM – The Stopping and Range of Ions in Matter* (2010), J. F. Ziegler, M. D. Ziegler and J. P. Biersack, Nucl.Instr. And Meth. B **268**, 1818-1823 (2010).

[17] L. Giuntini, M. Massi, S. Calusi, Nucl.Instr. and Meth. A. **576** (2007) 266-273